Available online at www.sciencedirect.com
ScienceDirect
Journal of Sound and Vibration 314 (2008) 53–69
JOURNAL OF SOUND AND VIBRATION
www.elsevier.com/locate/jsvi

Active vibration control based on linear matrix inequality for rotor system under seismic excitation

Yongjun Chen*, Changsheng Zhu

College of Electrical Engineering, Zhejiang University, Hangzhou 310027, Zhejiang, People's Republic of China

Received 21 April 2006; received in revised form 15 September 2007; accepted 5 January 2008
Handling Editor: L.G. Tham
Available online 20 February 2008

Abstract

For a flexible rotor system under seismic excitation, H_2, H_∞ and mixed H_2/H_∞ control strategies were formulated by means of linear matrix inequality (LMI) to attenuate the transient vibration of the flexible rotor system under a nonstationary seismic excitation and to improve robust performance of the flexible rotor system. A double-disc cantilever flexible rotor system was used as an example to verify the feasibility and the validity of the H_2, H_∞ and mixed H_2/H_∞ control strategies in active vibration control for a rotor system subjected to nonstationary El Centro seismic excitation. The performances of the rotor system in both frequency and time domains were analysed based on numerical optimization technique, which bases on an efficient convex optimization software. The feasibility and the effectiveness of the control strategies presented in active vibration control for a rotor system were verified. It is shown that for the H_∞ control, the displacement responses of the rotor system are effectively suppressed in the frequency domain, but transient-response performances are not so good. For the H_2 control, the transient responses of the rotor system attenuate quickly, but the frequency-response performances are not so good. The effectiveness of the mixed H_2/H_∞ control to suppress the displacement responses of the rotor system in the frequency domain and the transient response in time domain greatly depends on the H_∞ performance index. If the H_∞ performance index in the mixed H_2/H_∞ control is properly chosen, the mixed H_2/H_∞ control can effectively suppress both the displacement responses of the rotor system in the frequency domain and the transient response in time domain.
© 2008 Elsevier Ltd. All rights reserved.

1. Introduction

Lately, for most rotating machinery, such as turbines, compressors, machine tools and information storage devices, further performance enhancement is in demand in terms of speed, accuracy and reliable operation. Meanwhile, the rotating machinery is likely to face more severe vibrations caused by various vibration sources such as mass unbalance, shaft misalignment and exogenous disturbance. These vibrations are in turn responsible for not only performance degradations, but also excessive acoustic noises and fatigue-related damages. Therefore, the vibration suppression is a matter of great significance to rotating machinery systems. Two kinds of approaches, i.e., passive and active controls are often used. For a flexible rotor system which

*Corresponding author. Tel.: +86 571 8798 3515; fax: +86 571 8795 1625.
E-mail address: yjchenee@hotmail.com (Y. Chen).

0022-460X/$ - see front matter © 2008 Elsevier Ltd. All rights reserved.
doi:10.1016/j.jsv.2008.01.005

must pass through the several lateral bending critical speeds, it is impossible for the passive control system to select the stiffness and damping parameters so as to exert a significant influence over all these modes [1]. Therefore, the effectiveness of the passive vibration control is not very good, and the passive vibration control cannot meet the requirements of the high-performance rotational machinery. These limitations together with the desire to exercise greater control over rotor vibrations, with greatly enhanced performance, have led to a growing interest in the development of active vibration control of rotor systems.

Much work has been conducted in an effort to the active vibration control of rotor systems. Chen and Lee [2] presented a decoupling vibration control approach for a flexible rotor system with symmetric mass and stiffness matrices. Nonami et al. [3] reported an active control procedure for flexible rotors supported by magnetic bearings, but the gyroscopic effects were neglected. As it is well known, the gyroscopic effects have profound influence on the dynamic behaviour of rotor systems when operating at a high angular speed. Neglecting such effects may deteriorate the control system's performance or even invalidate the formulation. Furthermore, the presented decoupling procedure does not hold when the gyroscopic effects are considered. Lee and Chen [4] proposed an approach by designing a delicate feedback control to completely remove the gyroscopic effects, which then makes decoupling of the governing equations possible. However, Salm [5] found that the gyroscopic effects might serve to improve the system behaviour with large external damping. The complete removal of the gyroscopic effects by providing a counteractive control input to enable decoupling operation needs further justification. Burrows et al. [6] presented pole placement techniques for synchronous vibration control of a rotor-bearing system. Knospe et al. [7] presented three adaptive control algorithms and conducted experiments by using algorithms presented for unbalance response control of a rotor system and indicated that the advantages and disadvantages of each algorithm were illustrated by examining experimental results in a laboratory magnetic-bearing rotor rig. The rotor midspan vibration was almost completely eliminated over the operating rotational speed range. Considering characteristics of the fluid-film bearings, Abduljabbar et al. [8] presented an optimal controller to improve the dynamic behaviour of a flexible rotor system regarding resonance and instabilities. The effectiveness of the proposed controller in significantly improving rotor's performance in term of stabilization was demonstrated and desirable levels of vibration cancellation were achieved. Cole et al. [9] analysed active vibration control of a rotor system under direct forcing and base motion disturbances, in which the rotor contacting with retainer bushes was prevented with the proposed control approach. Recently, they applied frequency-matched control signals for control of multiple frequency components in active vibration control of the rotor system [10]. Yu et al. [11] given a detailed description of the electromagnetic actuator for active vibration control of a flexible rotor system and proposed a control algorithm based on the least-square method which can greatly reduced the synchronous vibrations of the rotor system. Keogh et al. [12] designed a transient vibration control strategy based on measured rotor's harmonic components and demonstrated the effectiveness of the control strategy in attenuating transient vibration control of the rotor system in mass loss case in a flexible rotor magnetic-bearing system. The problem of repeated contacts with the safety bush was alleviated and the transient vibration control was achieved effectively. Lin and Yu [13] presented a dual-level approach for modal vibration suppression of a rotor possessing repeated rigid-body modes with gyroscopic effects considered. The first level control of the approach presented is to remove any combination of flutter, divergence, rigid body and/or repeated modes by enabling positive definiteness of the augmented system, and the second level control is then applied for the augmented system with complex modes. A mode switching approach by directing control to the modes with higher vibration contribution can be beneficial in alleviating the higher mode residual vibration was demonstrated.

The researches mentioned above were focused on the active vibration control of rotor systems with exact dynamical model. However, there are always some uncertainties between the real model and the dynamical model of the rotor system. An H_∞ control with good frequency performance for modeling error and other uncertainties is used to overcome model uncertainty in rotor systems. Keogh et al. [14] presented an optimization approach based on the H_∞ norm to minimize the influence of forcing disturbances, modeling error and measurement error.

At present, almost researches in the active vibration control of rotor systems are concentrated on the deterministic excitation. In fact, in order to develop higher performance higher speed rotating machinery, the active vibration control of rotor system under deterministic excitations is not enough, the active vibration

control under random excitation, such as earthquake, should be studied. Stochastic optimal control, H_∞ control and H_2 control were used in active vibration control of random vibration. The stochastic optimal control cannot deal with the vibration system with modeling error and other uncertainties. However, the H_∞ control problems under random excitation were mainly focused on seismic vibration control of the structures or buildings [15–19]. Caruso et al. [20] presented the H_2 control technique and applied it to the vibration control of an elastic plate. Different H_2 control laws were designed and compared by simulation, in order to evaluate the performance obtained using different combinations of sensors and actuators together with models taking into account an increasing number of structural eigenmodes.

The H_∞ control is mainly concerned with frequency domain performances and does not guarantee good transient responses in the time domain for the controlled system. The H_2 control represents the optimal synthesis tool when the objective of the control is to minimize the vibration energy due to impulsive or stochastic disturbances acting on the controlled structure. The H_2 control gives more suitable performance on system transient responses in the time domain. In the active vibration control of flexible rotor system, it is necessary to realize both specifications of the time and the frequency domains. The mixed H_2/H_∞ control can satisfy both the time and the frequency domains performances of active vibration control problems in a practical sense.

The H_2 control and the H_∞ control could be solved in the frequency and the time domains. At present, the active vibration control of rotor system with the H_∞ control was solved by Riccati equation or inequality in the frequency domain. However, a lot of parameters and positive definite matrix must be regulated in solving the Riccati equation or inequality. Sometimes, the solution of the problem could not be found even if the problem has a solution. This brought much inconvenience for application in practice. Recently, efficient interior-point algorithms make it possible to solve the high-order linear matrix inequality (LMI) by the computer. And the LMI was widely used in control theory. The LMI approach can efficiently make up the deficiency of the Riccati equation approach mentioned above. The parameters and positive definite matrix need not be regulated in solving the LMI. Furthermore, the H_∞ control was transformed from the frequency domain to the time domain by the LMI approach. It is convenient to design the controller directly.

In general, the convexity is an important specification and many linear control problems can be reduced to convex optimization problems, which involve the LMI. The LMI has more flexibility for combining various design constraints on the controlled system. Recently, the LMI-based control system analysis has become popular since it encompasses many control subjects. The theory of the LMI-based control system analysis has been given as a very strict mathematical sense in Ref. [21]. However, very little work has been presented addressing the active vibration control based on the mixed H_2/H_∞ control. Nonami and Sivrioglu [22,23] applied the LMI-based mixed H_2/H_∞ control to investigate active vibration control for a structure. Fang et al. [24] developed an H_2/H_∞ control strategy for vehicle active suspension system. These researches considered the active vibration control under deterministic excitation. However, the study of the LMI-based mixed H_2/H_∞ control on active vibration control subjected to random excitation was not available yet.

In this study, the H_2, H_∞ and multiobjective H_2/H_∞ state feedback control strategies are described by means of the LMI and applied to active vibration control of the flexible rotor system under seismic excitation. The multiobjective H_2/H_∞ control problem is solved by using very efficient convex optimization software MALAB LMI Tools for a practical control object of the double-disc cantilever flexible rotor system under seismic excitation.

2. Mathematic model of a controlled rotor system under seismic excitation

The equation of motion of a linear unbalance rotor system under seismic excitation can be formulated as

$$\mathbf{M}\ddot{\mathbf{y}} + (\mathbf{G}+\mathbf{C})\dot{\mathbf{y}} + \mathbf{K}\mathbf{y} = \mathbf{F}\mathbf{U} + \mathbf{F}_u - \mathbf{M}\mathbf{E}\ddot{y}_g(t), \tag{1}$$

where $\mathbf{y}$, $\dot{\mathbf{y}}$ and $\ddot{\mathbf{y}}$ are generalized displacement, velocity and acceleration vectors of the rotor system, respectively. $\mathbf{M}$, $\mathbf{K}$ and $\mathbf{C}$ are mass, stiffness and damping matrices, respectively. $\mathbf{G}$ is a skew-symmetric angular speed-dependent gyroscopic matrix of the rotor system. $\mathbf{F}$ and $\mathbf{U}$ are control input matrix and control input vector, respectively. $\mathbf{F}_u$ is rotor's unbalance excitation force vector which is generally expressed as $\mathbf{F}_u = \mathbf{M}\mathbf{e}\Omega^2\mathbf{E}_u$ in the rotor system and $m_i e_i \Omega^2$ is the unbalance force at the ith node. m_i and e_i are mass and

rotor's unbalance eccentricity at the ith node, respectively. $\mathbf{E}_u$ is an indicated vector of the unbalance excitation force vector. $\mathbf{E}$ is an indicated vector of the inertial force and $\ddot{\mathbf{y}}_g(t)$ is acceleration of the ground random motion.

Letting $\mathbf{x}^{\mathrm{T}} = [\mathbf{y}^{\mathrm{T}} \quad \dot{\mathbf{y}}^{\mathrm{T}}]$, we can transform the second-order system equation (1) into a first-order system

$$\dot{\mathbf{x}} = \mathbf{A}\mathbf{x} + \mathbf{B}_1\mathbf{w} + \mathbf{B}_2\mathbf{u}, \tag{2}$$

where

$$\mathbf{A} = \begin{bmatrix} \mathbf{0} & \mathbf{I} \\ -\mathbf{M}^{-1}\mathbf{K} & -\mathbf{M}^{-1}(\mathbf{C}+\mathbf{G}) \end{bmatrix}, \quad \mathbf{B}_1 = \begin{bmatrix} \mathbf{0} & \mathbf{0} \\ \mathbf{0} & \mathbf{I} \end{bmatrix}, \quad \mathbf{B}_2 = \begin{bmatrix} \mathbf{I} & \mathbf{0} \\ \mathbf{0} & \mathbf{M}^{-1}\mathbf{F} \end{bmatrix}, \quad \mathbf{w} = \begin{bmatrix} \mathbf{0} \\ \mathbf{I}^{-1}\mathbf{M}^{-1}\mathbf{F}_u - \mathbf{E}\ddot{\mathbf{x}}_g(t) \end{bmatrix},$$

$$\mathbf{u} = \begin{Bmatrix} \mathbf{0} \\ \mathbf{U} \end{Bmatrix}.$$

Let us consider the following controlled output vector:

$$\mathbf{z} = \mathbf{C}_1\mathbf{x} + \mathbf{D}_{11}\mathbf{w} + \mathbf{D}_{12}\mathbf{u}. \tag{3}$$

The focus in active vibration control of the rotor system is to obtain control strategies that guarantee the stability of the closed-loop system and result in desirable performance by reducing the response of the rotor system due to the ground random motion and the unbalance excitation. The stability of the closed-loop system here means the standard notion of asymptotic stability (i.e., eigenvalues with strictly negative real parts for linear time-invariant systems).

For the performance, we seek to find the controllers that result in a controlled output (i.e., $\mathbf{z}$) that satisfies the following inequality, assuming zero initial conditions:

$$\int_0^\infty \mathbf{z}^{\mathrm{T}}\mathbf{z}\,\mathrm{d}t \leqslant \gamma^2 \int_0^\infty \mathbf{w}^{\mathrm{T}}\mathbf{w}\,\mathrm{d}t, \tag{4}$$

where γ which is a positive real number serves as the measure of performance, $\mathbf{w}$ is the disturbance signal (both acceleration excitation of ground random motion and rotor unbalance excitation) and $\mathbf{z}$ is the controlled output vector.

The standard definition of the L_2 norm of signal $\mathbf{z}$ is as follows:

$$\|\mathbf{z}\|_2^2 = \int_0^\infty \mathbf{z}^{\mathrm{T}}\mathbf{z}\,\mathrm{d}t. \tag{5}$$

Then, inequality (4) can be rewritten as

$$\|\mathbf{z}\|_2 \leqslant \gamma\|\mathbf{w}\|_2. \tag{6}$$

Hence, as γ becomes small, the effect of the disturbance on $\mathbf{z}$ is diminished. For time-invariant systems, the notation in inequality (6) is interchangeable with having the infinity norm of the transfer function from $\mathbf{w}$ to $\mathbf{z}$, $T_{\mathbf{zw}}$, be less than γ, i.e.,

$$\|T_{\mathbf{zw}}\|_\infty = \sup_{\mathbf{w}} \frac{\|\mathbf{z}\|_2}{\|\mathbf{w}\|_2} \leqslant \gamma. \tag{7}$$

3. Active vibration control strategies based on LMI

Let us consider the control structure shown in Fig. 1. It is assumed that the plant $\mathbf{G}$ is linear time invariant and the state vector $\mathbf{x}$ is measurable. Here, $\mathbf{w}$ denotes the exogenous input vector and $\mathbf{z}_\infty$ and $\mathbf{z}_2$ denote the controlled output vectors. The closed-loop transfer functions from $\mathbf{w}$ to $\mathbf{z}_\infty$ and $\mathbf{z}_2$ are, respectively, expressed as $T_{\mathbf{z}_\infty\mathbf{w}}$ and $T_{\mathbf{z}_2\mathbf{w}}$. The multiobjective H_2/H_∞ control strategy may be described as follows. Find a static state-feedback law $\mathbf{u} = \mathbf{K}\mathbf{x}$ such that $\|T_{\mathbf{z}_2\mathbf{w}}\|_2$ is minimized subject to $\|T_{\mathbf{z}_\infty\mathbf{w}}\|_\infty < \gamma$. This approach yields a

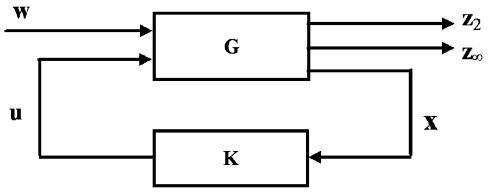

Fig. 1. Block diagram of H_2/H_∞ control system with state feedback.

convex sub-optimal control problem whose global minimum of the performance measure $J(T_{\mathbf{z}_2\mathbf{w}})$ is an upper bound on the optimal performance of transfer matrix $\|T_{\mathbf{z}_2\mathbf{w}}\|_2^2$.

The state space description of the control system shown in Fig. 1 is as follows:

$$\left.\begin{aligned}\dot{\mathbf{x}} &= \mathbf{A}\mathbf{x} + \mathbf{B}_1\mathbf{w} + \mathbf{B}_2\mathbf{u}\\ \mathbf{z}_\infty &= \mathbf{C}_1\mathbf{x} + \mathbf{D}_{11}\mathbf{w} + \mathbf{D}_{12}\mathbf{u}\\ \mathbf{z}_2 &= \mathbf{C}_2\mathbf{x} + \mathbf{D}_{21}\mathbf{w} + \mathbf{D}_{22}\mathbf{u}\end{aligned}\right\}, \tag{8}$$

where $\mathbf{x}$ is the state vector, $\mathbf{z}_\infty$ and $\mathbf{z}_2$ the controlled output vectors, $\mathbf{u}$ the control input and $\mathbf{w}$ the exogenous input. Supposing that the control input is a linear function of the state, i.e.,

$$\mathbf{u} = \mathbf{K}\mathbf{x}, \tag{9}$$

where $\mathbf{K}$ is the state feedback gain, the closed-loop system is given by

$$\left.\begin{aligned}\dot{\mathbf{x}} &= (\mathbf{A} + \mathbf{B}_2\mathbf{K})\mathbf{x} + \mathbf{B}_1\mathbf{w}\\ \mathbf{z}_\infty &= (\mathbf{C}_1 + \mathbf{D}_{12}\mathbf{K})\mathbf{x} + \mathbf{D}_{11}\mathbf{w}\\ \mathbf{z}_2 &= (\mathbf{C}_2 + \mathbf{D}_{22}\mathbf{K})\mathbf{x} + \mathbf{D}_{21}\mathbf{w}\end{aligned}\right\}. \tag{10}$$

3.1. H_2 control strategy

The H_2 norm of the transfer matrix $T_{\mathbf{z}_2\mathbf{w}}$ is finite if and only if $\mathbf{D}_{21} = 0$. In this case, the H_2 norm of the transfer matrix $T_{\mathbf{z}_2\mathbf{w}}$ is

$$\|T_{\mathbf{z}_2\mathbf{w}}\|_2^2 = \mathrm{Tr}\big((\mathbf{C}_2 + \mathbf{D}_{22}\mathbf{K})\mathbf{X}(\mathbf{C}_2 + \mathbf{D}_{22}\mathbf{K})^{\mathrm{T}}\big), \tag{11}$$

where the symmetric positive definite matrix $\mathbf{X}$ is obtained by solving the following Lyapunov equation:

$$(\mathbf{A} + \mathbf{B}_2\mathbf{K})\mathbf{X} + \mathbf{X}(\mathbf{A} + \mathbf{B}_2\mathbf{K})^{\mathrm{T}} + \mathbf{B}_1\mathbf{B}_1^{\mathrm{T}} = 0. \tag{12}$$

In general, the constraint is

$$\mathrm{Tr}(\mathbf{S}(\mathbf{x})\mathbf{P}^{-1}(\mathbf{x})\mathbf{S}^{\mathrm{T}}(\mathbf{x})) < \eta, \tag{13}$$

where $\mathbf{P}(\mathbf{x}) = \mathbf{P}^{\mathrm{T}}(\mathbf{x}) \in \mathbf{R}^{n\times n}$ and $\mathbf{S}(\mathbf{x}) \in \mathbf{R}^{p\times n}$, depending affinely on $\mathbf{x}$, is expressed by introducing a new matrix variable $\mathbf{M} = \mathbf{M}^{\mathrm{T}} \in \mathbf{R}^{p\times p}$, i.e., the LMI,

$$\mathrm{Tr}(\mathbf{M}) < \eta, \quad \begin{bmatrix} -\mathbf{M} & \mathbf{S}(\mathbf{x}) \\ \mathbf{S}^{\mathrm{T}}(\mathbf{x}) & -\mathbf{P}(\mathbf{x}) \end{bmatrix} < 0. \tag{14}$$

Letting $\mathbf{X}_2 = \mathbf{X}$, from the above expression, it can be shown that $\|T_{\mathbf{z}_2\mathbf{w}}\|_2^2$ is the minimum of $\mathrm{Tr}(\mathbf{Q})$ subject to

$$(\mathbf{A} + \mathbf{B}_2\mathbf{K})\mathbf{X}_2 + \mathbf{X}_2(\mathbf{A} + \mathbf{B}_2\mathbf{K})^{\mathrm{T}} + \mathbf{B}_1\mathbf{B}_1^{\mathrm{T}} < 0, \tag{15}$$

$$\begin{bmatrix} -\mathbf{Q} & (\mathbf{C}_2 + \mathbf{D}_{22}\mathbf{K})\mathbf{X}_2 \\ \mathbf{X}_2(\mathbf{C}_2 + \mathbf{D}_{22}\mathbf{K})^{\mathrm{T}} & -\mathbf{X}_2 \end{bmatrix} < 0, \tag{16}$$

$$\mathrm{Tr}(\mathbf{Q}) < \eta, \tag{17}$$

where $\mathbf{X}_2$ and $\mathbf{Q}$ are symmetric positive definite matrices, respectively.

In general, the linear quadratic performance objective of the optimal control is often used in control problems. Therefore, the linear quadratic performance objective should be transformed to the H_2 norm performance objective. Letting the linear quadratic performance objective be as follows:

$$J = \int_0^\infty (\mathbf{x}^{\mathrm{T}}\mathbf{Q}\mathbf{x} + \mathbf{u}^{\mathrm{T}}\mathbf{R}\mathbf{u})\,\mathrm{d}t \tag{18}$$

and introducing a reference signal $\mathbf{z}_2$

$$\mathbf{z}_2 = \begin{bmatrix} \mathbf{Q}^{1/2} \\ 0 \end{bmatrix}\mathbf{x} + \begin{bmatrix} 0 \\ \mathbf{R}^{1/2} \end{bmatrix}\mathbf{u}, \tag{19}$$

the linear quadratic performance objective (18) can be rewritten as

$$J = \int_0^\infty \mathbf{z}_2^{\mathrm{T}}\mathbf{z}_2\,\mathrm{d}t = \left\|T_{\mathbf{z}_2\mathbf{w}}\right\|_2^2. \tag{20}$$

In this way, the linear quadratic performance objective of the optimal control is transformed to the H_2 performance objective of the transfer function from the disturbance $\mathbf{w}$ to the reference signal $\mathbf{z}_2$. The matrices $\mathbf{C}_2$ and $\mathbf{D}_{22}$ in Eq. (8) should be $[\mathbf{Q}^{1/2\mathrm{T}} \quad 0^{\mathrm{T}}]^{\mathrm{T}}$ and $[0^{\mathrm{T}} \quad \mathbf{R}^{1/2\mathrm{T}}]^{\mathrm{T}}$, respectively.

3.2. H_∞ control strategy

The bounded real lemma plays a central role in obtaining the H_∞ constraint. There exists a quadratic Lyapunov function $\mathbf{V}(\mathbf{x}) = \mathbf{x}\mathbf{P}\mathbf{x}$ such that for all time t,

$$\frac{\mathrm{d}}{\mathrm{d}t}\mathbf{V}(\mathbf{x}) + \mathbf{z}_\infty^{\mathrm{T}}\mathbf{z}_\infty - \gamma^2\mathbf{w}^{\mathrm{T}}\mathbf{w} < 0, \tag{21}$$

where $\mathbf{P}$ is a symmetric positive definite matrix.

Substituting Eq. (10) into inequality (21), we obtained the following inequality:

$$\begin{aligned}&[(\mathbf{A}+\mathbf{B}_2\mathbf{K})\mathbf{x} + \mathbf{B}_1\mathbf{w}]^{\mathrm{T}}\mathbf{P}\mathbf{x} + \mathbf{x}^{\mathrm{T}}\mathbf{P}[(\mathbf{A}+\mathbf{B}_2\mathbf{K})\mathbf{x} + \mathbf{B}_1\mathbf{w}] \\ &\quad + [(\mathbf{C}_1+\mathbf{D}_{12}\mathbf{K})\mathbf{x} + \mathbf{D}_{11}\mathbf{w}]^{\mathrm{T}}[(\mathbf{C}_1+\mathbf{D}_{12}\mathbf{K})\mathbf{x} + \mathbf{D}_{11}\mathbf{w}] - \gamma^2\mathbf{w}^{\mathrm{T}}\mathbf{w} < 0.\end{aligned} \tag{22}$$

By rearrangement of inequality (22), using the Schur complement [21], the following inequality can be obtained:

$$\begin{bmatrix} (\mathbf{A}+\mathbf{B}_2\mathbf{K})^{\mathrm{T}}\mathbf{P} + \mathbf{P}(\mathbf{A}+\mathbf{B}_2\mathbf{K}) + (\mathbf{C}_1+\mathbf{D}_{12}\mathbf{K})^{\mathrm{T}}(\mathbf{C}_1+\mathbf{D}_{12}\mathbf{K}) & \mathbf{P}\mathbf{B}_1 + (\mathbf{C}_1+\mathbf{D}_{12}\mathbf{K})^{\mathrm{T}}\mathbf{D}_{11} \\ \mathbf{B}_1^{\mathrm{T}}\mathbf{P} + \mathbf{D}_{11}^{\mathrm{T}}(\mathbf{C}_1+\mathbf{D}_{12}\mathbf{K}) & -\gamma^2\mathbf{I} + \mathbf{D}_{11}^{\mathrm{T}}\mathbf{D}_{11} \end{bmatrix} < 0. \tag{23}$$

Using the Schur complement for inequality (23) and multiplying by $\mathbf{P}^{-1}$ from right and left, we obtain

$$\begin{aligned}&\mathbf{P}^{-1}(\mathbf{A}+\mathbf{B}_2\mathbf{K})^{\mathrm{T}} + (\mathbf{A}+\mathbf{B}_2\mathbf{K})\mathbf{P}^{-1} + \mathbf{P}^{-1}(\mathbf{C}_1+\mathbf{D}_{12}\mathbf{K})^{\mathrm{T}}(\mathbf{C}_1+\mathbf{D}_{12}\mathbf{K})\mathbf{P}^{-1} \\ &\quad - \left[\mathbf{B}_1 + \mathbf{P}^{-1}(\mathbf{C}_1+\mathbf{D}_{12}\mathbf{K})^{\mathrm{T}}\mathbf{D}_{11}\right](-\gamma^2\mathbf{I} + \mathbf{D}_{11}^{\mathrm{T}}\mathbf{D}_{11})^{-1}\left[\mathbf{B}_1^{\mathrm{T}} + \mathbf{D}_{11}^{\mathrm{T}}(\mathbf{C}_1+\mathbf{D}_{12}\mathbf{K})^{\mathrm{T}}\mathbf{P}^{-1}\right] < 0.\end{aligned} \tag{24}$$

By putting it in the LMI form again, we have

$$\begin{bmatrix} \begin{pmatrix} (\mathbf{A}+\mathbf{B}_2\mathbf{K})\mathbf{P}^{-1} + \mathbf{P}^{-1}(\mathbf{A}+\mathbf{B}_2\mathbf{K})^{\mathrm{T}} \\ +\mathbf{P}^{-1}(\mathbf{C}_1+\mathbf{D}_{12}\mathbf{K})^{\mathrm{T}}(\mathbf{C}_1+\mathbf{D}_{12}\mathbf{K})\mathbf{P}^{-1} \end{pmatrix} & \mathbf{B}_1 + \mathbf{P}^{-1}(\mathbf{C}_1+\mathbf{D}_{12}\mathbf{K})^{\mathrm{T}}\mathbf{D}_{11} \\ \mathbf{B}_1^{\mathrm{T}} + \mathbf{D}_{11}^{\mathrm{T}}(\mathbf{C}_1+\mathbf{D}_{12}\mathbf{K})\mathbf{P}^{-1} & -\gamma^2\mathbf{I} + \mathbf{D}_{11}^{\mathrm{T}}\mathbf{D}_{11} \end{bmatrix} < 0. \tag{25}$$

Multiplying inequality (25) by diag[$\gamma^{1/2}\mathbf{I}$ $\gamma^{-1/2}\mathbf{I}$] from right and left, and letting variable $\mathbf{X}_\infty = \gamma\mathbf{P}^{-1}$, the following inequality can be obtained:

$$\begin{bmatrix} (\mathbf{A}+\mathbf{B}_2\mathbf{K})\mathbf{X}_\infty + \mathbf{X}_\infty(\mathbf{A}+\mathbf{B}_2\mathbf{K})^{\mathrm{T}} & \mathbf{B}_1 \\ \mathbf{B}_1^{\mathrm{T}} & -\gamma\mathbf{I} \end{bmatrix} + \frac{1}{\gamma}\begin{bmatrix} \mathbf{X}_\infty(\mathbf{C}_1+\mathbf{D}_{12}\mathbf{K})^{\mathrm{T}} \\ \mathbf{D}_{11}^{\mathrm{T}} \end{bmatrix}\begin{bmatrix} (\mathbf{C}_1+\mathbf{D}_{12}\mathbf{K})\mathbf{X}_\infty & \mathbf{D}_{11} \end{bmatrix} < 0. \tag{26}$$

Using the Schur complement again, the following inequality can be obtained as the H_∞ constraint of the closed-loop system (10) for $\mathbf{X}_\infty > 0$:

$$\begin{bmatrix} (\mathbf{A}+\mathbf{B}_2\mathbf{K})\mathbf{X}_\infty + \mathbf{X}_\infty(\mathbf{A}+\mathbf{B}_2\mathbf{K})^{\mathrm{T}} & \mathbf{B}_1 & \mathbf{X}_\infty(\mathbf{C}_1+\mathbf{D}_{12}\mathbf{K})^{\mathrm{T}} \\ \mathbf{B}_1^{\mathrm{T}} & -\gamma\mathbf{I} & \mathbf{D}_{11}^{\mathrm{T}} \\ (\mathbf{C}_1+\mathbf{D}_{12}\mathbf{K})\mathbf{X}_\infty & \mathbf{D}_{11} & -\gamma\mathbf{I} \end{bmatrix} < 0. \tag{27}$$

3.3. The mixed H_2/H_∞ control strategy

The H_2 and H_∞ control strategies based on the LMI were derived above, respectively. Now we will combine these two constraints into one design expression. The mixed H_2/H_∞ control problem is to minimize the H_2 norm of $T_{\mathbf{z}_2\mathbf{w}}$ over all state feedback gains $\mathbf{K}$ such that what also satisfies the H_∞ norm constraint. On the other hand, inequalities (15), (16) and (27) are not convex because of the nonlinear terms $\mathbf{K}\mathbf{X}_2$ and $\mathbf{K}\mathbf{X}_\infty$. The convexity condition requires a common Lyapunov matrix such that

$$\mathbf{X} = \mathbf{X}_2 = \mathbf{X}_\infty. \tag{28}$$

With the new variable $\mathbf{W} = \mathbf{K}\mathbf{X}$, the multiobjective H_2/H_∞ control using H_2 and H_∞ performance constraints can be given by minimizing $\mathrm{Tr}(\mathbf{Q})$ over $\mathbf{X} = \mathbf{X}^{\mathrm{T}}$, $\mathbf{Q} = \mathbf{Q}^{\mathrm{T}}$ and $\mathbf{W}$ subject to

$$\begin{bmatrix} \mathbf{A}\mathbf{X}+\mathbf{B}_2\mathbf{W}+(\mathbf{A}\mathbf{X}+\mathbf{B}_2\mathbf{W})^{\mathrm{T}} & \mathbf{B}_1 & (\mathbf{C}_1\mathbf{X}+\mathbf{D}_{12}\mathbf{W})^{\mathrm{T}} \\ \mathbf{B}_1^{\mathrm{T}} & -\gamma\mathbf{I} & \mathbf{D}_{11}^{\mathrm{T}} \\ \mathbf{C}_1\mathbf{X}+\mathbf{D}_{12}\mathbf{W} & \mathbf{D}_{11} & -\gamma\mathbf{I} \end{bmatrix} < 0, \tag{29}$$

$$\begin{bmatrix} -\mathbf{Q} & \mathbf{C}_2\mathbf{X}+\mathbf{D}_{22}\mathbf{W} \\ (\mathbf{C}_2\mathbf{X}+\mathbf{D}_{22}\mathbf{W})^{\mathrm{T}} & -\mathbf{X} \end{bmatrix} < 0, \tag{30}$$

$$\mathrm{Tr}(\mathbf{Q}) < \eta. \tag{31}$$

After finding of a solution ($\mathbf{X}$, $\mathbf{Q}$ and $\mathbf{W}$) to this multiobjective control problem, the optimal feedback control law of control system (8) is obtained as

$$\mathbf{u} = \mathbf{W}\mathbf{X}^{-1}\mathbf{x}. \tag{32}$$

4. Seismic excitation model and acceleration of the ground random motion

The El Centro seismic excitation is used here. When the acceleration of the ground random motion is denoted as $\ddot{w}(t)$, the power spectral density of the El Centro seismic excitation can be expressed approximately by

$$S_{\ddot{w}}(\omega) = \frac{S_c\omega^2}{(a^4+\omega^4)(b^2+\omega^2)} \quad -\infty < \omega < \infty, \tag{33}$$

where $a = 10\pi$ rad/s, $b = 2\pi$ rad/s and $S_c = 3.55\times10^4\,\mathrm{m^2/s^3}$.

Generally, the seismic excitation is nonstationary and must be considered as nonstationary stochastic process. The power spectral density of seismic excitation is time dependent and can be expressed as

$$S_{\ddot{w}}(\omega, t) = g(t)S_{\ddot{w}}(\omega), \tag{34}$$

where $g(t)$ is a slowly varying envelope function. In this paper, $g(t)$ is formulated as follows:

$$g(t) = \frac{t}{2} e^{(1-t/2)}. \tag{35}$$

The method of Monte Carlo simulation is employed to determine acceleration of the ground random motion $\ddot{\mathbf{y}}_g(t)$. For a rotor system subjected to random excitations with a given power spectral density $S_{\ddot{w}}(\omega)$, the time history of the spectral function $S_{\ddot{w}}(\omega)$ can be numerically simulated by using a series of trigonometric functions, i.e.,

$$\ddot{\mathbf{y}}_g(t) = g(t) \sum_{k=1}^{N} A_k \cos(\omega_k t + \varphi_k), \tag{36}$$

where N is the total number of frequency points, A_k the amplitude, ω_k the circular frequency of each term in the trigonometric series, φ_k the uniformly random variable between 0 and 2π and φ_j and φ_k are independent of each other if $i \neq j$. A_k and ω_k can be obtained by

$$A_k^2 = 4 S_{\ddot{w}}(\omega_k) \Delta\omega, \tag{37}$$

$$\omega_k = \omega_l + (k - 1/2)\Delta\omega, \tag{38}$$

where $S_{\ddot{w}}$ is the power spectral density function of the stochastic process, ω_u and ω_l are the upper and the lower limits of frequency concerned, respectively. $\Delta\omega = (\omega_u - \omega_l)/N$ is frequency interval and $k = 1,2,\ldots,N$, where N is a natural number.

5. Numerical example and analysis

Generally, there is no analytical solution to the LMIs, but they can be solved by numerical methods. The above inequalities are solved using the efficient convex optimization software MATLAB LMI Toolbox.

A double-disc flexible rotor system shown in Fig. 2 was used as an example to verify the feasibility and the validity of the H_2, H_∞ and mixed H_2/H_∞ control strategies in active vibration control for the flexible rotor system subjected to seismic excitation. The double-disc cantilever flexible rotor system is located in the horizontal plane. One side of the rotor was supported on a rigid bearing and the other on a flexible bearing. The geometric size and physical parameters of the double-disc cantilever flexible rotor system are the distance between the rigid bearing and disc A, l_1, is 0.2 m; the distance between disc A and the flexible bearing, l_2, is 0.15 m and distance between the flexible bearing and disc B, l_3, is 0.1 m; the radii of the flexible shaft, disc A and disc B are 0.03, 0.15 and 0.09 m, respectively; the thicknesses of disc A and disc B are 0.05 and 0.03 m, respectively; the unbalance eccentricities of both discs e are 10×10^{-6} m; Yong's modulus of the material of the shaft E is 2×10^{11} N/m^2; mass density of the disc ρ is 7850 kg/m^3; the lumped mass of the flexible bearing is 2 kg; the steady angular speed of the rotor is 500 rad/s which is much greater than the first critical angular

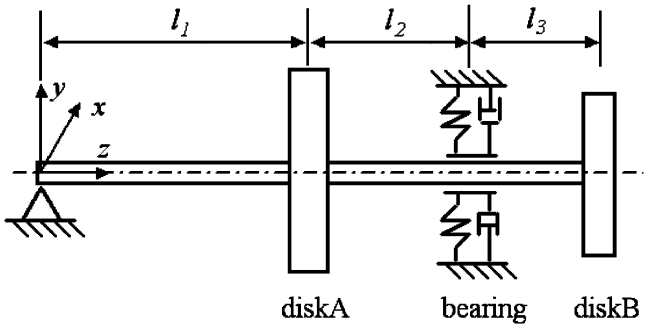

Fig. 2. Schematic of a double-disc cantilever flexible rotor system.

speed 238 rad/s. At the steady operational angular speed, the stiffness coefficients and damping coefficients of the flexible bearing are, respectively, as follows:

$$\begin{bmatrix} k_{xx} & k_{xy} \\ k_{yx} & k_{yy} \end{bmatrix} = \begin{bmatrix} 1.87\times10^{6} & 4.10\times10^{5} \\ 4.10\times10^{5} & 1.87\times10^{6} \end{bmatrix} \text{N/m},$$

$$\begin{bmatrix} c_{xx} & c_{xy} \\ c_{yx} & c_{yy} \end{bmatrix} = \begin{bmatrix} 1.6\times10^{2} & 2.10\times10^{2} \\ 2.10\times10^{2} & 1.5\times10^{2} \end{bmatrix} \text{N s/m}.$$

The double-disc cantilever flexible rotor system is simplified to a massless elastic shaft with two rigid discs and a lumped mass at the flexible-bearing location. It is a rotor system with ten degree of freedom. The equation of motion of the rotor system under seismic excitation can be obtained easily by using the lumped-parameter method.

The steady unbalance displacement response of the double-disc cantilever flexible rotor system at different angular speeds is shown in Fig. 3, which is obtained through calculating steady amplitudes of the rotor system at different steady angular speeds. The unbalance displacement response of disc B is mostly larger than that of disc A. It is shown that there are four peaks on the unbalance response at the angular speeds of 238, 315, 483 and 569 rad/s, respectively, which correspond to the first four critical angular frequencies of the double-disc cantilever flexible rotor system, i.e., 238.6, 314.8, 483.4 and 569.6. The first three peaks are very evident, but the fourth peak is not evident.

It is assumed that the displacements of the discs are measurable and there are a seismic excitation and an unbalance excitation on the rotor system. The displacement sensors and the actuators are configured in both the horizontal and vertical directions for discs A and B. Then, the state space mode of the controlled double-disc cantilever flexible rotor system can be formulated as follows:

$$\left.\begin{aligned} \dot{\mathbf{x}} &= \mathbf{A}\mathbf{x} + \mathbf{B}_1\mathbf{w} + \mathbf{B}_2\mathbf{u} \\ \mathbf{z}_\infty &= \mathbf{C}_1\mathbf{x} \\ \mathbf{z}_2 &= \mathbf{C}_2\mathbf{x} + \mathbf{D}_{22}\mathbf{u} \end{aligned}\right\}, \tag{39}$$

where $\mathbf{x} = [x_{d1}\ y_{d1}\ \theta_{xd1}\ \theta_{yd1}\ x_{d2}\ y_{d2}\ \theta_{xd2}\ \theta_{yd2}\ x_b\ y_b\ \dot{x}_{d1}\ \dot{y}_{d1}\dot{\theta}_{xd1}\ \dot{\theta}_{yd1}\ \dot{x}_{d2}\ \dot{y}_{d2}\ \dot{\theta}_{xd2}\ \dot{\theta}_{yd2}\ \dot{x}_b\ \dot{y}_b]^{\mathrm{T}}$ is the state vector, $\mathbf{z}_\infty$ and $\mathbf{z}_2$ are the controlled output vectors determined by the H_∞ and the H_2 performance objectives, respectively. Matrices $\mathbf{A}$, $\mathbf{B}_1$ and $\mathbf{B}_2$ are determined by the physical parameters of the rotor system

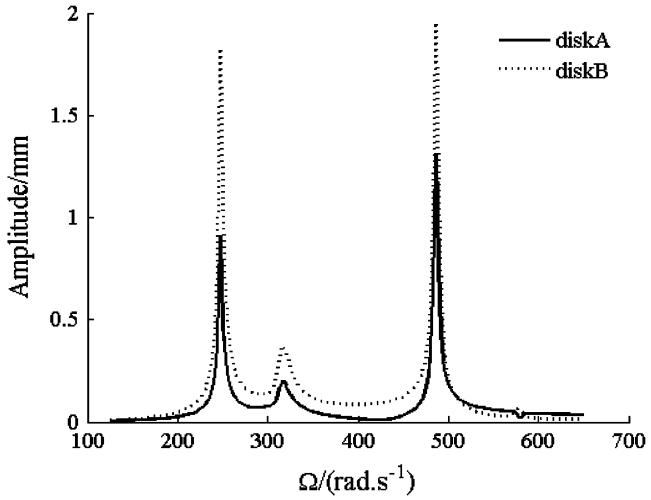

Fig. 3. Steady unbalance response of the rotor system.

and controlled input and output according to Eq. (2):

$$\mathbf{C}_1 = \begin{bmatrix} 0_{1\times10} & 1 & 0 & 0 & 0 & 0 & 0 & 0_{1\times4} \\ 0_{1\times10} & 0 & 1 & 0 & 0 & 0 & 0 & 0_{1\times4} \\ 0_{1\times10} & 0 & 0 & 0 & 0 & 1 & 0 & 0_{1\times4} \\ 0_{1\times10} & 0 & 0 & 0 & 0 & 0 & 1 & 0_{1\times4} \end{bmatrix}, \quad \mathbf{C}_2 = \mathbf{I}_{20\times20}, \quad \mathbf{D}_{22} = \begin{bmatrix} 1 & 0 & 0 & 0 & 0 & 0 & 0_{1\times14} \\ 0 & 1 & 0 & 0 & 0 & 0 & 0_{1\times14} \\ 0 & 0 & 0 & 0 & 1 & 0 & 0_{1\times14} \\ 0 & 0 & 0 & 0 & 0 & 1 & 0_{1\times14} \end{bmatrix}^{\mathrm{T}}.$$

The power spectral density of El Centro seismic acceleration is shown in Fig. 4. The frequency corresponding to the peak value of the power spectral density is 2.57 Hz. The energy of the seismic wave mainly exists in the lower frequency region. Time history of the acceleration of the El Centro earthquake is shown in Fig. 5. It is shown that the magnitude of peak value of the acceleration is 3.12 m/s^2.

In the active vibration control of a flexible rotor system, both performances in the frequency domain and the time domain should be considered. The simulation results about the frequency-response curve and the transient-response time history under impulse load of the flexible rotor system are mainly analysed. The displacement response of the flexible rotor system in the frequency domain is obtained by transfer matrix method. The transient response of the flexible rotor system in the time domain is obtained by Duhamel integration under impulse load. The results in the x-direction and the y-direction are similar due to the symmetry of the double-disc cantilever flexible rotor system. Therefore, the numerical results in the x-direction are used to show the effectiveness of active vibration control for the double-disc cantilever flexible rotor system based on the H_∞, H_2 and mixed H_2/H_∞ controls.

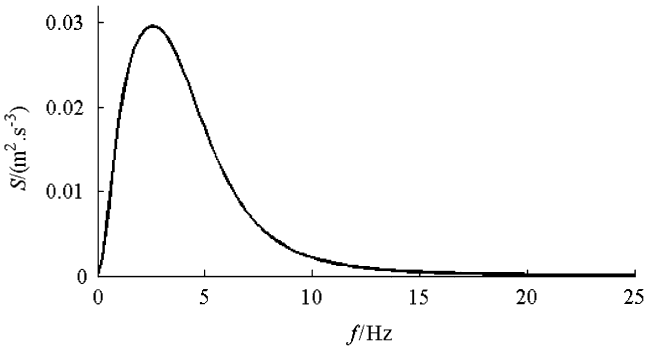

Fig. 4. PSD of the acceleration of the El Centro earthquake.

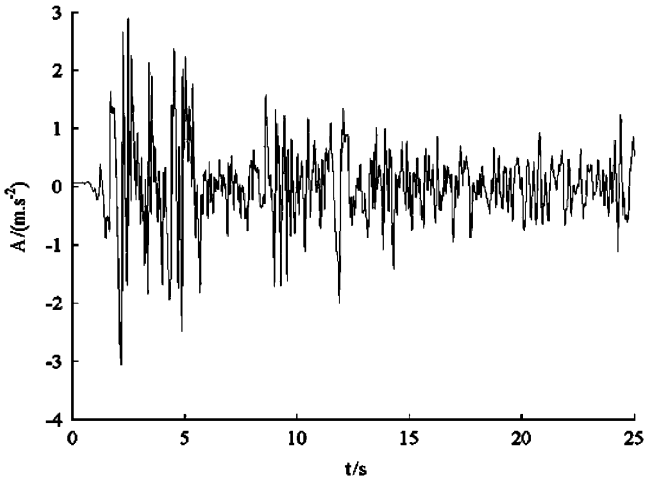

Fig. 5. Time history of the acceleration of the El Centro earthquake.

With and without the H_∞ control, the frequency responses and the transient responses in the x-direction of discs A and B of the double-disc cantilever flexible rotor system under El Centro seismic excitation are shown in Figs. 6–9, respectively. Without the H_∞ control, there are five peaks on the frequency-response curves in Figs. 6 and 8, which are corresponded to the first five critical angular frequencies of the rotor system, i.e., 238, 315, 483, 569 and 839 rad/s, respectively. The peaks on the frequency-response curves of the rotor system almost disappear with the H_∞ control and the vibrations of the rotor system in the critical angular speed regions are completely suppressed. Without the H_∞ control, transient responses in the time domain attenuate slowly in Figs. 7 and 9. The transient responses of the discs attenuate quickly with the H_∞ control, but the transient-response performances are not so good and the transient response to decay takes a long time. The frequency response of disc B is larger than that of disc A and the locations of the peaks are same without the H_∞ control. The vibrations of the both discs are effectively suppressed in the critical angular speed regions with the H_∞ control. Similarly, the transient response of disc B is larger than that of disc A without the H_∞ control. The transient responses of both discs attenuate with the H_∞ control.

With and without the H_2 control, the frequency and the transient responses of disc A under El Centro seismic excitation are shown in Figs. 10 and 11, respectively. Without the H_2 control, there are five peaks on

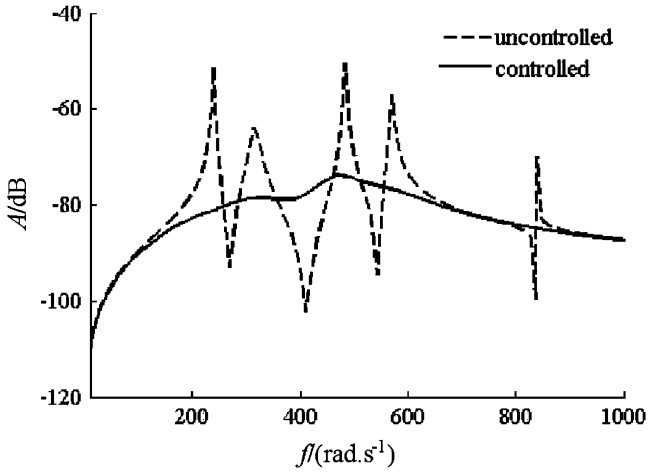

Fig. 6. Frequency response of disc A with the H_∞ control.

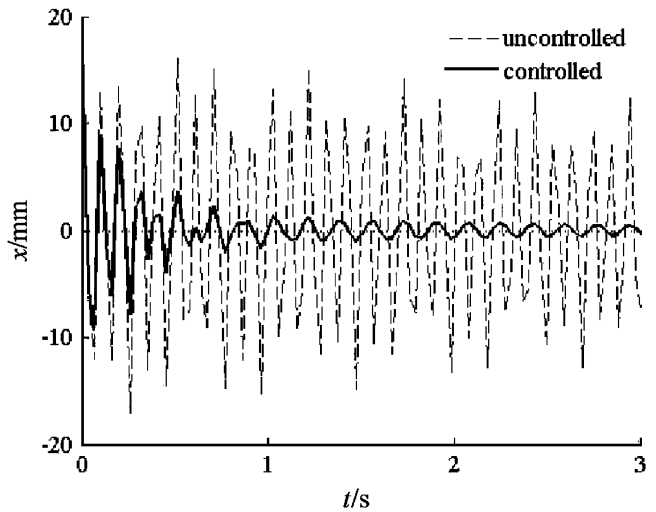

Fig. 7. Impulse response of disc A with the H_∞ control.

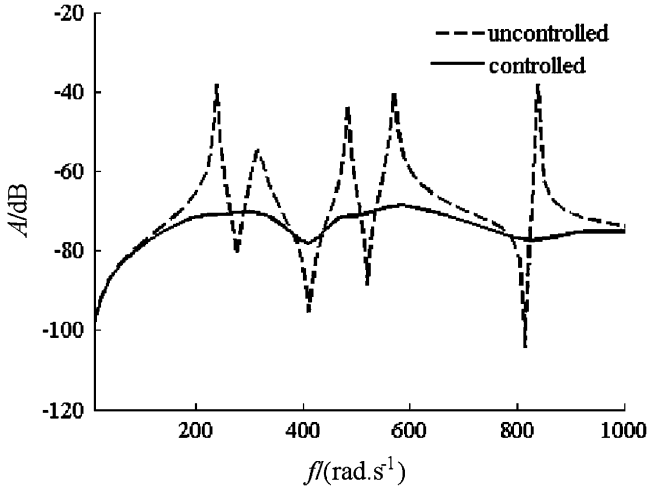

Fig. 8. Frequency response of disc B with the H_∞ control.

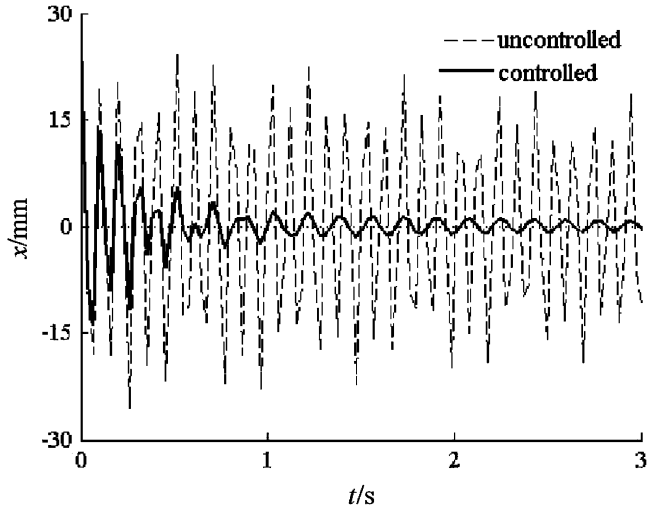

Fig. 9. Impulse response of disc B with the H_∞ control.

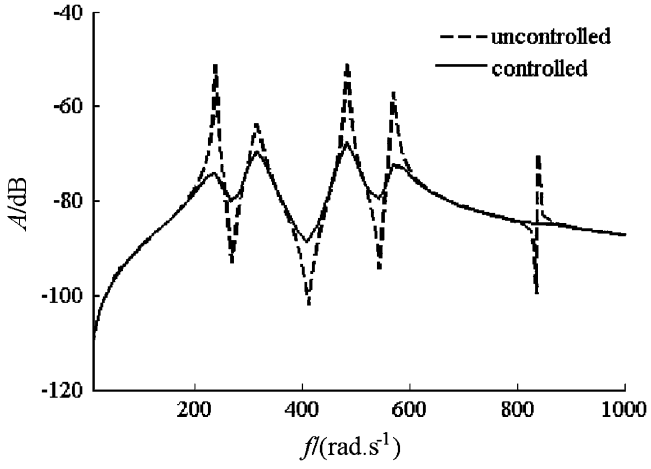

Fig. 10. Frequency response of disc A with the H_2 control.

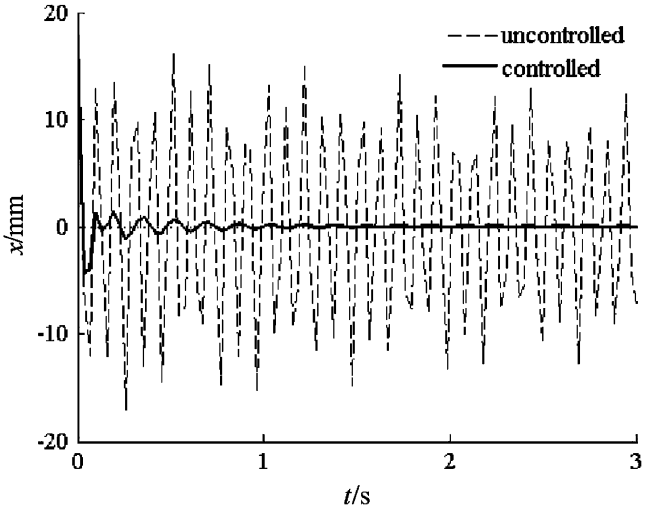

Fig. 11. Impulse response of disc A with the H_2 control.

the frequency response in Fig. 10. The vibration of disc A are suppressed in the critical angular speed regions in some extent with the H_2 control, but the frequency-response performance is not so good. The transient response of disc A attenuates slowly without the H_2 control and the transient response of disc A attenuates very quickly with the H_2 control in Fig. 11. The transient response of disc A attenuates completely after half-second.

In the mixed H_2/H_∞ control, the H_∞ performance index γ has a great effect on the control effectiveness. From Eq. (7), we know that γ is the supermum of the root mean square gain for the transfer function $T_{\mathbf{zw}}$ from the exogenous disturbance to the controlled output, which denotes the effects of the exogenous disturbance on the controlled output. Therefore, the H_∞ performance index γ is determined by the exogenous disturbance in the practical design. The smaller the H_∞ performance index γ is, the better the control effectiveness is in theory. The main factor considering in choosing the H_∞ performance index γ is the exogenous disturbance in practice. In Ref. [18], the peak value of the seismic acceleration is 7.29 m/s^2, γ is selected as 0.125, the desired performance is guaranteed. The seismic excitation combined with the rotor unbalance excitation as the exogenous disturbance of the double-disc cantilever flexible rotor system was considered. The maximum equivalent acceleration due to the seismic excitation and the rotor unbalance is smaller than 7.29 in our analysis, so $\gamma = 0.125$ is chosen in our analysis in order to guarantee the desired performance of the double-disc cantilever flexible rotor system.

When $\gamma = 0.125$, with and without the H_2/H_∞ control, the frequency response and the transient response of disc A under El Centro seismic excitation are shown in Figs. 12 and 13, respectively. It is shown that there are five peaks on the frequency response without the H_2/H_∞ control and the peaks disappear on the frequency response of disc A with the mixed H_2/H_∞ control. The displacement response of disc A is effectively suppressed in the frequency domain and the control effectiveness is quite good for this case. The transient response of disc A attenuates slowly without the mixed H_2/H_∞ control and the transient response of disc A attenuates very quickly with the mixed H_2/H_∞ control. The transient response of disc A with the mixed H_2/H_∞ control attenuates more quickly than that with the pure H_∞ control in Figs. 7 and 9 and completely attenuates after half-second. Therefore, the improvement of the time response of the rotor system due to introduction of the H_2 control in the H_∞ control is very obvious.

The frequency responses and the transient responses of disc A with the mixed H_2/H_∞ control under different H_∞ performance indices γ are shown in Figs. 14–19, respectively. It is shown that the effectiveness of the mixed H_2/H_∞ control on the displacement responses of disc A at the critical frequency regions greatly depends on the H_∞ performance index γ. As the H_∞ performance index γ in the mixed H_2/H_∞ control increases, the displacements of disc A at the critical frequency regions in the frequency-response curves increase obviously and the transient response of disc A attenuates slowly. The control effectiveness of the

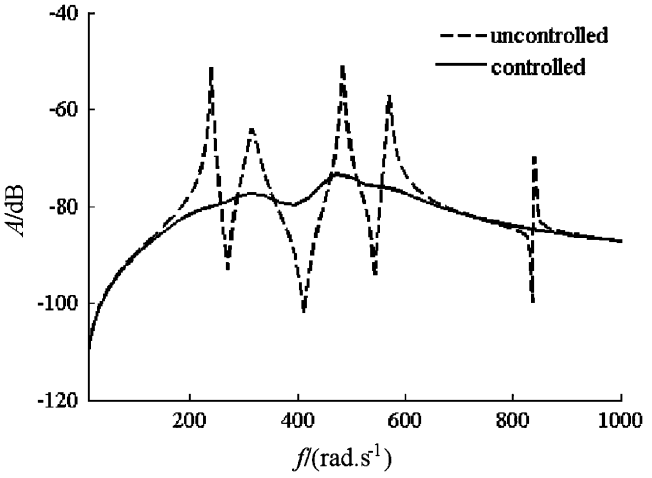

Fig. 12. Frequency response of disc A with mixed H_2/H_∞ control.

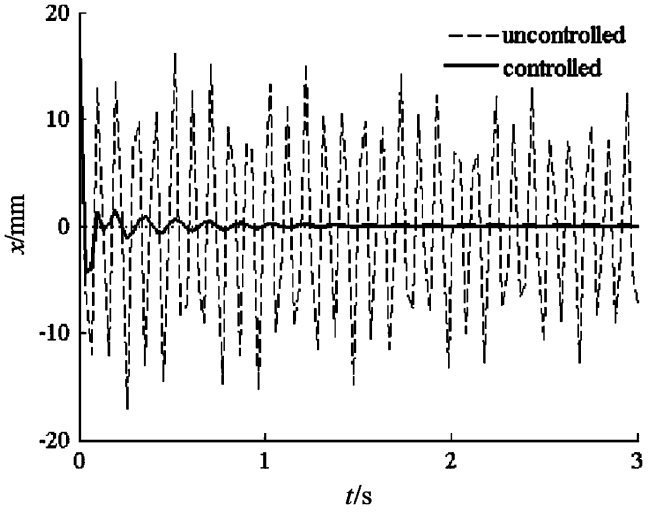

Fig. 13. Impulse response of disc A with the mixed H_2/H_∞ control.

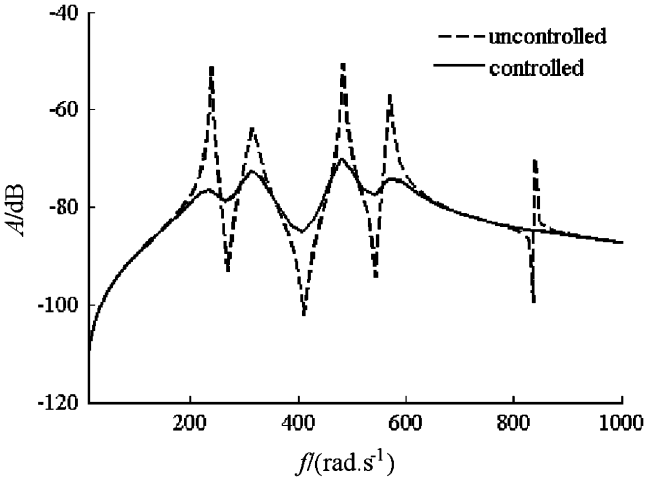

Fig. 14. Frequency response of disc A with the mixed H_2/H_∞ control for $\gamma = 0.25$.

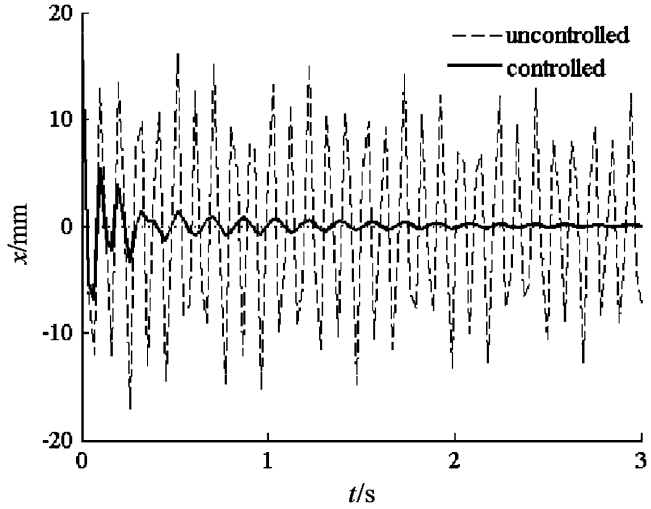

Fig. 15. Impulse response of disc A with the mixed H_2/H_∞ control for $\gamma = 0.25$.

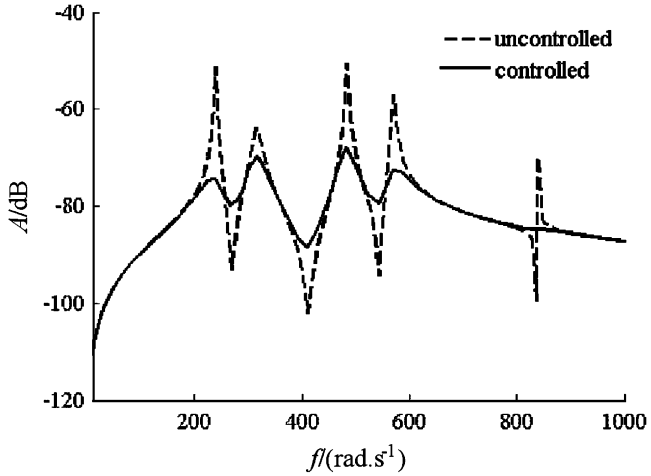

Fig. 16. Frequency response of disc A with the mixed H_2/H_∞ control for $\gamma = 0.5$.

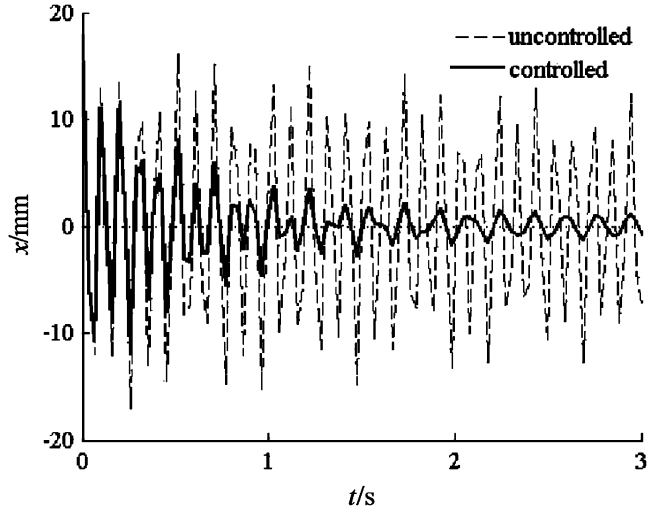

Fig. 17. Impulse response of disc A with the mixed H_2/H_∞ control for $\gamma = 0.5$.

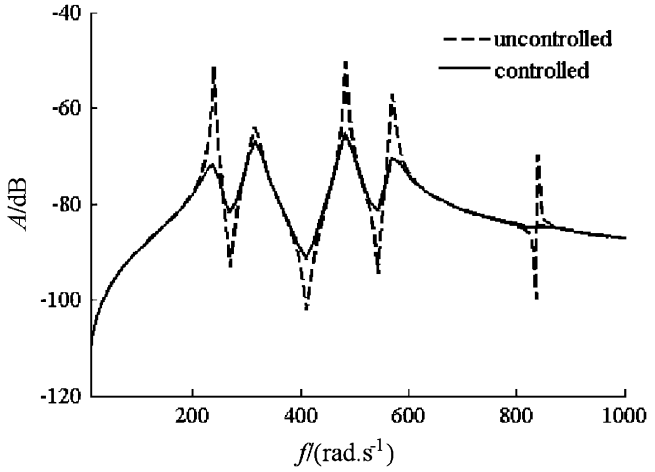

Fig. 18. Frequency response of disc A with the mixed H_2/H_∞ control for $\gamma = 1$.

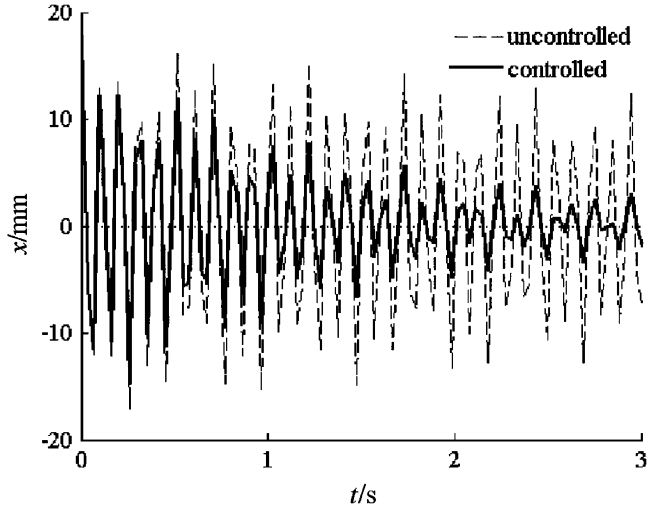

Fig. 19. Impulse response of disc A with the mixed H_2/H_∞ control for $\gamma = 1$.

mixed H_2/H_∞ control to disc A becomes worse with an increase of H_∞ performance index γ in both the frequency and the time domains. Therefore, a small feasible H_∞ performance index γ should be selected in practical active vibration control design of the flexible rotor system.

6. Conclusions

The H_2, H_∞ and mixed H_2/H_∞ control strategies were formulated, respectively, by means of the LMI. An active vibration control for a double-disc cantilever flexible rotor system under seismic excitation were analysed by the H_2, H_∞ and mixed H_2/H_∞ control strategies, respectively. It is shown that for the H_∞ control, the displacement responses of a rotor system in the frequency domain are effectively suppressed at the critical angular frequencies regions of a rotor system, but the transient-response performances are not so good. For the H_2 control, the transient responses of the discs attenuate very quickly, but the frequency-response performances are not so good. For the mixed H_2/H_∞ control, the control effectiveness depends on the H_∞ performance index. The effectiveness of the mixed H_2/H_∞ control to the rotor systems becomes worse with increment of H_∞ performance index. If the H_∞ performance index is properly chosen, the mixed H_2/H_∞

control can effectively suppress both the displacement responses of a rotor system in the frequency domain and the transient vibration of a rotor system in time domain.

Acknowledgements

This research is supported by the key project of the National Natural Science Foundation of China under Grant nos. 10332030 and 10472101. The supports are gratefully acknowledged.

References

[1] R. Stanway, C.R. Burrows, Active vibration control of a flexible rotor on flexibly-mounted journal bearings, *Journal of Dynamic Systems, Measurement and Control—Transactions of the ASME* 103 (4) (1981) 383–388.
[2] S.T. Chen, A.C. Lee, Decoupling vibration control of a flexible rotor system with symmetric mass and stiffness properties, *Proceedings of the Institution of Mechanical Engineers* 207 (1) (1993) 9–14.
[3] K. Nonami, T. Yamanaka, M. Tominaga, Vibration and control of a flexible rotor supported by magnetic bearings, *JSME International Journal Series III* 33 (4) (1990) 475–482.
[4] A.C. Lee, S.T. Chen, Optimal vibration control for a flexible rotor with gyroscopic effects, *JSME International Journal Series III* 35 (3) (1992) 446–455.
[5] J.R. Salm, Active electromagnetic suspension of an elastic rotor: modeling, control, and experimental results, *Journal of Vibration, Acoustics, Stress, and Reliability in Design* 110 (4) (1988) 493–500.
[6] C.R. Burrows, P.S. Keogh, R. Tasaltin, Closed-loop vibration control of flexible rotors—an experimental study, *Proceedings of the Institution of Mechanical Engineers, Part C: Journal of Mechanical Engineering Science* 207 (1) (1993) 1–17.
[7] C.R. Knospe, R.W. Hope, S.J. Fedigan, R.D. Williams, Experiments in the control of unbalance response using magnetic bearings, *Mechatronics* 5 (4) (1995) 385–400.
[8] Z. Abduljabbar, M.M. ElMadany, A.A. AlAbdulwahab, Active vibration control of a flexible rotor, *Computers and Structures* 58 (3) (1996) 499–511.
[9] M.O.T. Cole, P.S. Keogh, C.R. Burrows, Vibration control of a flexible rotor/magnetic bearing system subject to direct forcing and base motion disturbances, *Proceedings of the Institution of Mechanical Engineers, Part C: Journal of Mechanical Engineering Science* 212 (7) (1998) 535–546.
[10] M.O.T. Cole, P.S. Keogh, C.R. Burrows, Control of multifrequency rotor vibration components, *Proceedings of the Institution of Mechanical Engineers, Part C: Journal of Mechanical Engineering Science* 216 (2) (2002) 165–178.
[11] Z. Yu, L.T. Meng, L.M. King, Electromagnetic bearing actuator for active vibration control of a flexible rotor, *Proceedings of the Institution of Mechanical Engineers, Part C: Journal of Mechanical Engineering Science* 212 (8) (1998) 705–716.
[12] P.S. Keogh, M.O.T. Cole, C.R. Burrows, Multi-state transient rotor vibration control using sampled harmonics, *Journal of Vibration and Acoustics* 124 (2) (2002) 186–197.
[13] Yih-Hwang Lin, Hsiang-Chieh Yu, Active modal control of a flexible rotor, *Mechanical Systems and Signal Processing* 18 (2004) 1117–1131.
[14] P.S. Keogh, C. Mu, C.R. Burrows, Optimized design of vibration controllers for steady and transient excitation of flexible rotors, *Proceedings of the Institution of Mechanical Engineers, Part C: Journal of Mechanical Engineering Science* 209 (3) (1995) 155–168.
[15] F. Jabbari, W.E. Schmitendorf, J.N. Yang, H_{infinity} control for seismic-excited buildings with acceleration feedback, *Journal of Engineering Mechanics* 121 (9) (1995) 994–1002.
[16] J.G. Chase, H.A. Smith, Robust H_{infinity} control considering actuator saturation I: theory, *Journal of Engineering Mechanics* 122 (10) (1996) 976–983.
[17] J.G. Chase, H.A. Smith, S. Tetsuo, Robust H_{infinity} control considering actuator saturation II: applications, *Journal of Engineering Mechanics* 122 (10) (1996) 984–993.
[18] J.G. Chase, S.E. Breneman, H.A. Smith, Robust H_{infinity} static output feedback control with actuator saturation, *Journal of Engineering Mechanics* 125 (2) (1999) 225–233.
[19] Sheng-Guo Wang, P.N. Roschke, H.Y. Yeh, Simulation of robust control for uncertain structural systems against earthquakes, *Proceedings of the Fourth World Congress on Intelligent Control and Automation*, Vol. 3, Shanghai, June 2002, pp. 1681–1686.
[20] G. Caruso, S. Galeani, L. Menini, Active vibration control of an elastic plate using multiple piezoelectric sensors and actuators, *Simulation Modelling Practice and Theory* 11 (2003) 403–419.
[21] G.E. Dullerud, F. Paganini, *A Course in Robust Control Theory—A Convex Approach*, Springer, New York, 2000.
[22] K. Nonami, S. Sivrioglu, Active vibration control using LMI-based mixed H_2/H_∞ state and output feedback control with nonlinearity, *Proceedings of the 35th Conference on Decision and Control*, Kobe, February 1996, pp. 161–166.
[23] S. Sivrioglu, K. Nonami, Active vibration control by means of LMI-based mixed H_2/H_{inf} state feedback control, *JSME International Journal Series C* 40 (2) (1997) 239–244.
[24] Min Fang, Ying Wang, Wu-wei Chen, Mixed H_2/H_∞ control & μ analysis of vehicle active suspension system, *Proceedings of the Fifth World Congress on Intelligent Control and Automation*, Hangzhou, June 2004, pp. 723–727.